

UCRL--86954

DE82 004389

HIGH-FRAME-RATE NEUTRON RADIOPHOTOGRAPHY  
OF DYNAMIC EVENTS

R. H. Bossi  
A. H. Robinson  
J. P. Barton

MASTER

This paper was prepared for submittal to the  
Proceedings of the World Conference on Neutron  
Radiography, San Diego, CA, December 7-10, 1981

November 20, 1981

This is a preprint of a paper intended for publication in a journal or proceedings. Since changes may be made before publication, this preprint is made available with the understanding that it will not be cited or reproduced without the permission of the author.

Lawrence  
Livermore  
National  
Laboratory

DISCLAIMER

This work was performed under the auspices of the U.S. Department of Energy by Lawrence Livermore National Laboratory under contract No. W-7405-Eng-48.

## HIGH-FRAME-RATE NEUTRON RADIOGRAPHY OF DYNAMIC EVENTS\*

R. H. Bossi<sup>†</sup>, A. H. Robinson and J. P. Barton<sup>\*\*</sup>  
Oregon State University  
Corvallis, Oregon, U.S.A.

A system has been developed to perform neutron radiographic analysis of dynamic events having a duration of several milliseconds. The system has been operated in the range of 2000 to 10,000 frames/second. Synchronization has provided high-speed-motion neutron radiographs for evaluation of the firing cycle of 7.62 mm munition rounds within a steel rifle barrel. The system has also been used to demonstrate the ability to produce neutron radiographic movies of two phase flow.

The equipment uses the Oregon State University TRIGA reactor capable of pulsing to 3000 MW peak power, a neutron beam collimator, a scintillator neutron conversion screen coupled to an image intensifier, and a 16 mm high speed movie camera. The peak neutron flux incident at the object position is approximately  $4 \times 10^{11} \text{ n/cm}^2\text{s}$  with a pulse, full width at half maximum, of 9 ms.

Special studies have been performed on the scintillator conversion screens and on the effects of statistical limitations on the image quality. Modulation transfer function analysis has been used to assist in the evaluation of the system performance.

### INTRODUCTION

This paper describes the development of a technique that enables the neutron radiographic analysis of dynamic processes over a period lasting from one to ten milliseconds. The key to the technique is the use of a neutron pulse that is broad enough to span the duration of the brief event of interest, and intense enough to permit recording of the results on a high speed movie film at frame rates to 10,000 frames/second. Applications of this high-speed-motion neutron radiography system have been in ballistic studies and two phase flow.

\*This work was performed under the auspices of the U.S. Department of Energy by Lawrence Livermore National Laboratory under contract No. W-7405-Eng-48.

<sup>†</sup>Lawrence Livermore National Laboratory, P.O. Box 808, Livermore, California 94550, U.S.A.

<sup>\*\*</sup>Consultant, La Jolla, California, U.S.A.

eb

## SYSTEM DESIGN

The high-speed-motion neutron radiography system design incorporates a pulsing reactor, a beam collimator with limited loss of neutron intensity, and a scintillator screen imaging system [1-3]. The light from the scintillator screen is input to an image intensifier, and the information is recorded by a high speed photographic movie camera focused on the intensifier output. This system is illustrated in Fig. 1.

The neutron source is the Oregon State University TRIGA Mark II reactor. It has the capability of pulsing to 3000 MW peak power with about 9 ms full width at half maximum. The neutron intensity is not a constant throughout the pulse and therefore the images experience a gradual variation of exposure from frame to frame according to the pulse shape.

The neutron beam collimator is located on a tangential beam port of the reactor. This provides a neutron to gamma ratio and cadmium ratio that are superior to a standard radial beam port. At the object location the L/D ratio, measured by geometric unsharpness, is 30 in the horizontal direction and 41 in the vertical direction. The neutron flux at the object location is  $1.4 \times 10^5$  n/cm<sup>2</sup>s/kW. At 3000 MW, peak pulsing power, this yields  $4.2 \times 10^{11}$  n/cm<sup>2</sup>s. The gold cadmium ratio is 2.24 and the neutron radiographic beam purity is N75-10, as measured for gadolinium foil and Kodak SR film using the ASTM indicator. A fine collimator and masking, just around the area of interest in the object, are used in the experiments to reduce scatter from the object and surrounding material.

The collimated neutron beam passes through the object being radiographed and is detected by a scintillator screen. Lithium fluoride-zinc sulphide scintillators, with the lithium enriched in the <sup>6</sup>Li isotope, are normally used. The images created by the scintillation process are amplified by a two stage, 40 mm diameter ITT image intensifier. The 40 mm diameter input size limits the field size of the radiographic image. The radiant power gain measured by the manufacturer is a factor of 332 for the two combined stages and the resolution is 35 line pairs/mm. The image intensifier is coupled to the scintillator by pressure contact of the flat scintillator surface to the flat fiber-optic input surface of the intensifier. The intensifier photocathode and phosphor materials must be selected to avoid persistence problems at the required frame rates. An S-20 photocathode, having good spectral matching to the ZnS scintillator, and a P-11 output phosphor are used.

The final stage of the system is the high speed camera and film. A Hycam model K20S 4E rotating prism camera is focused on the output face-plate of the intensifier. The camera operates with 120 m rolls of 16 mm film at up to 11,000 frames/second, although it is normally run with 38 m rolls which limit the fastest frame rate to about 8000 frames/second. The rotating prism system uses a camera shutter factor of 2.5 which means that at 5000 frames/second the exposure per frame is  $1/(2.5 \times 5000) = 80 \mu\text{s}$ . A variety of 16 mm films have been compared for this system and those selected for most applications are the Kodak RAR 2496 and 2498 films.

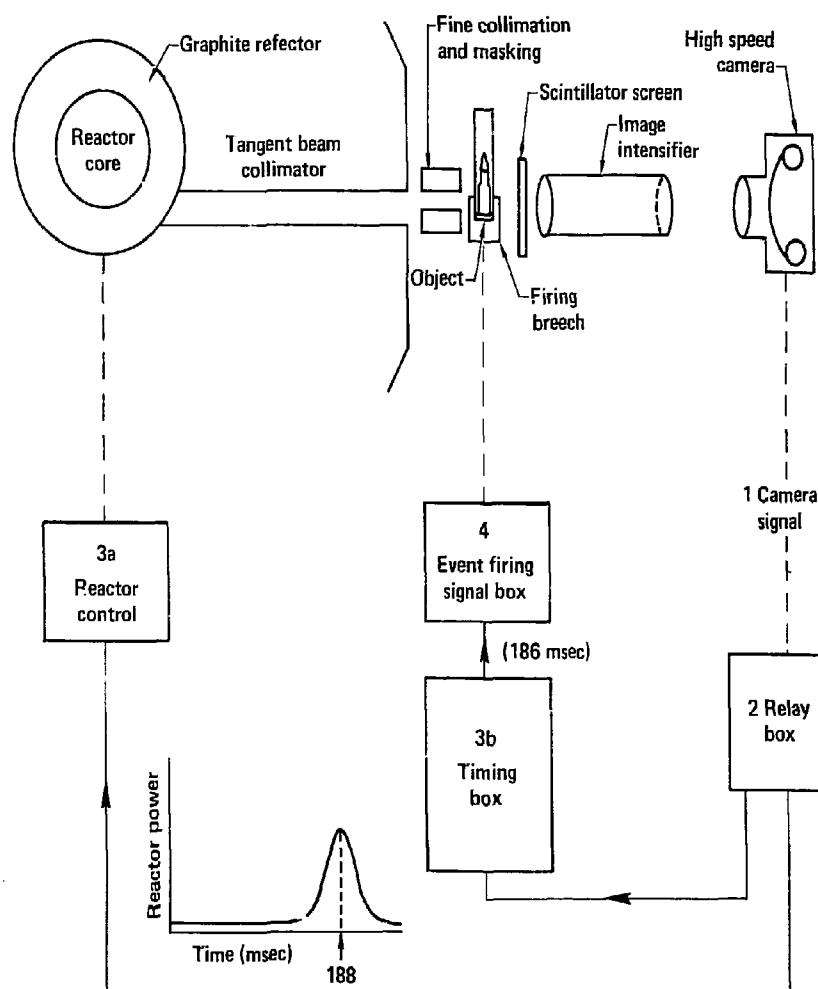


Figure 1. Diagram of the high-speed-motion neutron radiography system and the synchronization with a munition round object.

The synchronization system used for ordnance device high-speed-motion neutron radiography is shown as part of Fig. 1. A timing process is used once the camera reaches the desired speed. The time from the TRIGA transient rod initiation to peak power is 188 ms  $\pm$  4.8 ms (95% confidence) from a 100 W starting level. The event can therefore be satisfactorily timed to coincide with the peak neutron flux at the object.

### TYPICAL RESULTS

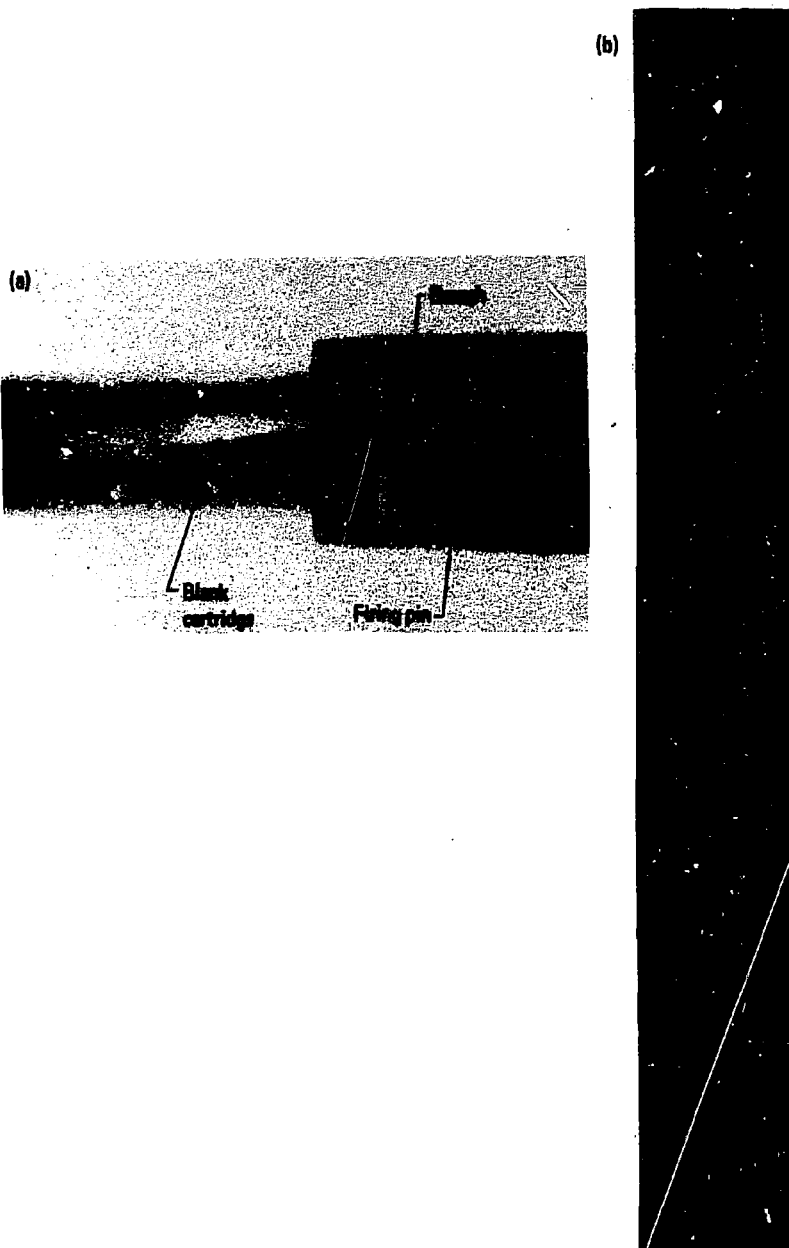
This system has been used to study the ballistic cycle of 7.62 mm rifle shells. Fig. 2a shows a high quality stationary neutron radiograph of a blank cartridge in a rifle barrel with a firing breech in place. The blank is only partially filled with powder. The contrast between the neutron opaque propellant and the void region above it can be clearly seen. The breech is shown with the firing pin in the central cavity slightly back from the breech faceplate. A gas igniter system, operating on an electrical signal, fills the cavity generating a pressure which forces the firing pin into the primer on the cartridge. The region of interest for the high-speed-motion neutron radiography is the rectangular area of the powder bed alone. The rest is masked by the fine collimation.

Fig. 2b shows one of the more than 250 high-speed-motion neutron radiography experiments performed on the ballistic cycle. Reproduction has reduced the detail visibility and density latitude of the original, but major features remain. This figure contains the sequential frames of the blank being fired with the high speed camera operating at 2000 frames/second. A 2600 MW pulse with about a 9 ms width was used. The powder lies flat across the imaged area. As the firing is initiated the bed humps up in several locations and is then consumed relatively evenly. The burning sequence covers about 2 to 2.5 ms.

Fig. 3a shows the firing sequence of another blank cartridge viewed near the primer. The overlap of the breech threaded onto the barrel is imaged. The frame rate is 5000 frames/second. Figure 3b shows a full cartridge radiographed at 8000 frames/second. The top of the powder line is detected in the first three frames and then is lost as the burn begins. The burn covers about eight frames (1 ms). Figure 3c is a full cartridge radiographed at 5000 frames/second. Gadolinium oxide has been added to two of the powder grains in the upper left of the image to improve the sensitivity. The tagged grains can be observed to move to the left and disappear during the firing. This enhancement technique has been used in a number of tests to detect individual grain movement. The black dot in frame six is an artifact. Recoil of the barrel is evident in both of the full cartridge firing sequences.

### SCINTILLATOR COMPARISON

A variety of scintillator screens have been tested for application in the high-speed-motion neutron radiography system. The necessary qualities are good resolution for use in the transmission orientation, good statistical efficiency, good light yield, and rapid decay characteristics. An experimental comparison of scintillators is shown in Table 1.



**Figure 2. (a) Neutron radiograph of a 7.62 mm munition round blank in a rifle barrel.**

**(b) High-speed-motion neutron radiograph of the powder burn inside the rifle barrel.**

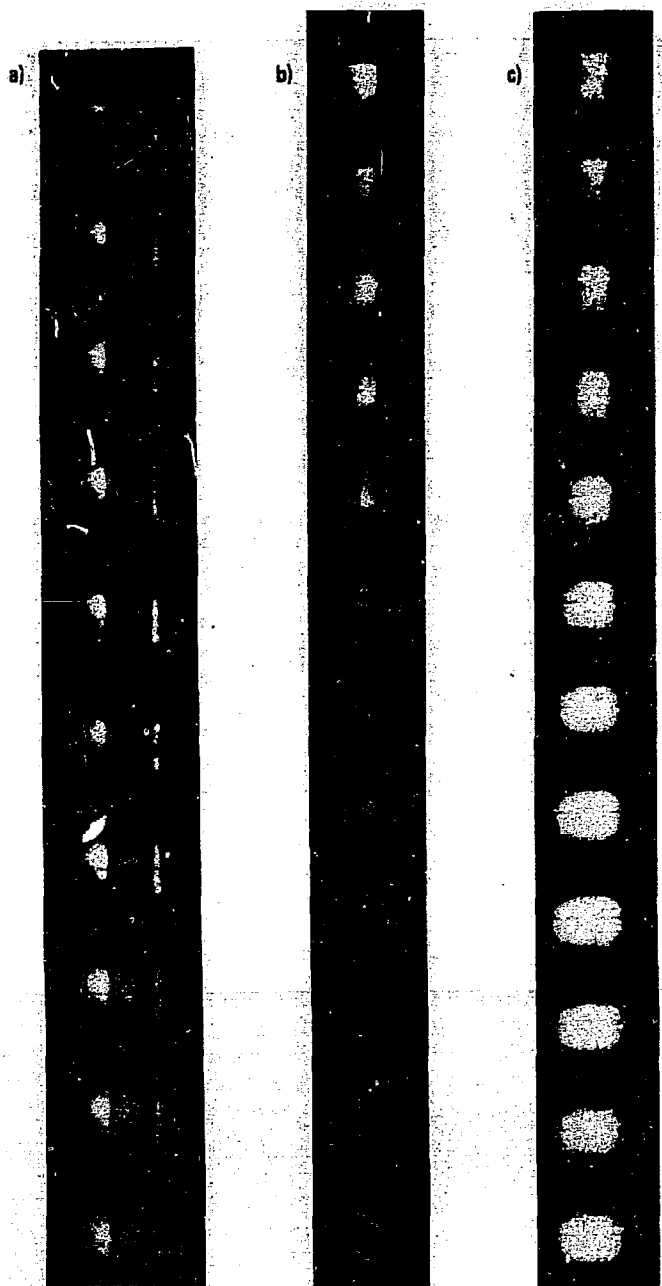


**Figure 3. High-speed-motion neutron radiographs of a) blank cartridge at 5000 frames/second,  
b) full cartridge at 8000 frames/second and  
c) full cartridge at 5000 frames/second with two grains of powder doped with gadolinium oxide.**

Table 1. Experimental Comparison of Scintillator Screen Types

Type (thickness)	Manufacturer	Relative Light Yield	Image Quality <sup>a</sup>
Gd <sub>2</sub> O <sub>2</sub> S	Apex Research	25	A
Gd <sub>2</sub> OBr:Er (0.1 mm)	General Electric Co.	10	B
Gd <sub>2</sub> O <sub>2</sub> S:Tb (0.06 mm)	Lockheed, Palo Alto, Ca	10	B
Ce-glass (1.0 mm)	Nuclear Enterprises (905)	70	D
LiF-ZnS (0.24 mm)	Oregon State University	50	D
LiF-ZnS (0.18 mm)	Nuclear Enterprises (425)	45	D
LiF-ZnS (0.24 mm)	C.E.N. Grenoble	40	D
LiF-ZnS (0.31 mm)	Nuclear Enterprises (425)	30	D
LiF-ZnS (0.1 mm)	Oregon State University	20	D
LiF-ZnS (0.2 mm)	Paisley College, Scotland	100	E
LiF-ZnS (0.1 mm)	Nuclear Enterprises (A)	20	E
<sup>10</sup> B-ZnS	Nuclear Enterprises (402)	12	E
<sup>10</sup> B-ZnS	Oregon State University	12	G

a)Number of details distinguished on the VISQI [4] test object:  
 A = 65, B = 60, C = 55, D = 45, E = 45, F = 40, and G = 35.

Rare earth scintillators of gadolinium oxysulphide and gadolinium oxybromide demonstrate the highest inherent resolution but have large light decay constants (on the order of 400  $\mu$ s) making them unsuitable for high frame rate imaging. Glass scintillators have short decay constants on the order of 40 to 60 ns. Unfortunately, tests show them to have low light yield and poor image quality when used in the transmission mode.

Zinc sulphide (ZnS) containing neutron scintillators have light decay characteristics composed of two components: a fast component having a decay constant on the order of 40 to 100 ns and a slower component on the order of 40 to 100  $\mu$ s. These scintillators may be made with a mixture of <sup>6</sup>LiF and ZnS or <sup>10</sup>B and ZnS [5-8]. The <sup>10</sup>B containing scintillators tested have demonstrated both a poor light yield and poor image quality. The <sup>6</sup>LiF-ZnS scintillators have been found to have the greatest light yield, sufficiently rapid light decay characteristics, and good image quality in the transmission mode.

#### STATISTICAL LIMITATIONS

Since the high-speed-motion system operates with high efficiency scintillators and light amplification, the radiographic image is formed with a minimal neutron signal. In this instance it becomes possible that the image quality can be limited due to the statistical fluctuation of the neutron signal itself. This statistical limitation problem may be experimentally evaluated by replacing the high speed camera in Fig. 1 with a 35 mm camera. The reactor is operated in the steady state mode at low power and the camera shutter is opened for extended periods to integrate the exposure. Since the image intensifier provides light amplification the film will receive suitable exposure in a reasonable time. The film

exposure is adjustable by the integrated neutron exposure and the f-stop setting on the 35 mm camera. The effect of the change in f-stop of the camera lens on the image quality is minimal because it has a resolution capability far beyond the scintillator screen.

Table 2 lists the results of the VISQI test object radiographed at exposures of 10 kW-min ( $10^8$  n/cm<sup>2</sup>) down to 0.1 kW-min ( $10^6$  n/cm<sup>2</sup>) with three LiF-ZnS scintillators fabricated at Oregon State University. The film densities are fairly consistent within each scintillator exposure set. The table values consist of the number of sensitivity factors detected on the first two steps of the VISQI. It is clear that as the neutron exposure is decreased the ability to discern detail is diminished. This occurs around 1 kW-min or  $10^7$  n/cm<sup>2</sup> incident fluence.

Table 2. VISQI Sensitivity Readings  
For Neutron Statistics Comparison

Exposure	Scintillator #57		Scintillator #56		Scintillator #54	
	2/1 ZnS to LiF 0.13 mm thick	density sensitivity	2/1 ZnS to LiF 0.24 mm thick	density sensitivity	4/1 ZnS to LiF 0.13 mm thick	density sensitivity
10 kW-min	1.58	34.5	1.69	35.5	1.54	35.5
3 kW-min	1.66	34.5	1.61	37	1.64	35
1 kW-min	1.59	33	1.54	36	1.56	33.5
.3 kW-min	1.53	32	1.56	35	1.56	30.5
.1 kW-min	1.57	23.5	1.57	31.5	1.45	21

#### SYSTEM EVALUATION

The high-speed-motion imaging system has been evaluated for image quality by modulation transfer function (MTF) analysis [9-13]. The MTF is the Fourier transform of the imaging system's one dimensional line spread function, and allows the evaluation of the individual as well as combined effects of the components by the commutative properties.

The MTF's were obtained by using an edge scan technique. A sharp edge of a 0.03 mm thick gadolinium foil was radiographed with the high-speed-motion system. The radiograph was scanned with a microdensitometer and the data numerically differentiated to obtain the line spread function and Fourier transformed to obtain the MTF. The computer routine performs the differentiation and transformation using a cubic spline interpolation of the data to generate the line spread function in terms of an interpolating polynomial from which the exact cosine and sine transforms are calculated. The image intensifier, high speed camera, and RAR 2498 film were similarly evaluated using the image of the edge of a razor blade for the edge scan. The results are shown in Fig. 4. The effect of the scintillator to make the complete high-speed-motion neutron imaging system is clearly indicated.

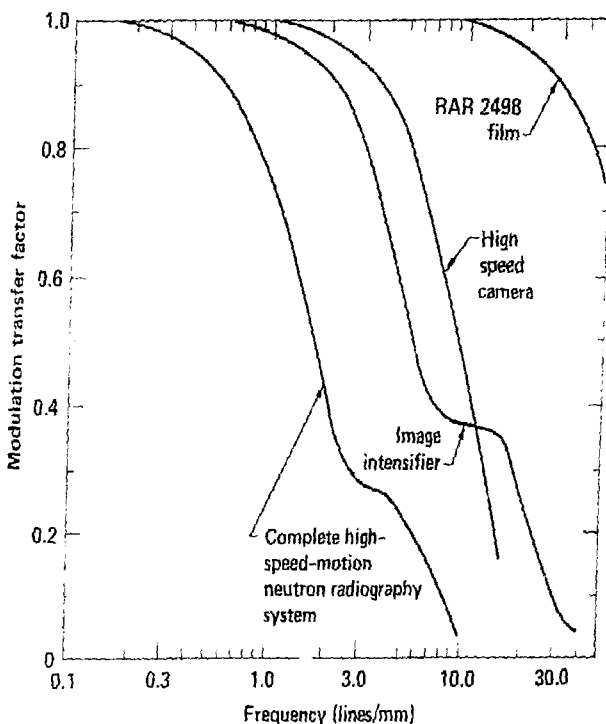


Figure 4. Modulation transfer functions for the high-speed-motion neutron radiography system evaluation.

#### ACKNOWLEDGMENT

We would like to thank Frankford Arsenal for their support in part of this work.

#### REFERENCES

- [1] Robinson, A.H., Barton, J.P., Trans. Amer. Nuc. Soc. 15 (1972) 140.
- [2] Bossi, R.H., thesis, Oregon State University (1976).
- [3] Barton, J.P., Bossi, R.H., Robinson, A.H., Ch. 14, Proc. Flash Radiography Symposium (Bryant, L.E., Jr., Ed.) ASNT (1977).
- [4] Barton, J.P., J. of Mat. 7 1 (1972) 18.
- [5] Spowart, A.R., Brit. J. Nondes. Test. 3 (1962) 2.
- [6] Wang, S.P., et. al., Rev. Sci. Inst. 33 (1962) 126.
- [7] Udyavar, R.S., B.A.R.C. 649, India, (1972).
- [8] Bossi, R.H., Robinson, A.H., Trans. Amer. Nuc. Soc. 22 (1975) 153.
- [9] Mees, C.E., James, T.H., Eds., The Theory of the Photographic Process, MacMillan Co. New York (1967) 507.
- [10] Hawksworth, M.R., Raoof, M.S., J. of Phys. E. 3 (1970) 851.
- [11] Bossi, R.H., et. al., Mat. Eval. 30 5 (1972) 103.
- [12] Alder, D.M., Bull S.R., Trans. Amer. Nuc. Soc. 22 (1975) 145.
- [13] Bossi, R.H., Robinson, A.H., Trans. Amer. Nuc. Soc. 26 (1977) 157.